A photovoltaic source I/U model suitable for hardware in the loop application

ROBERT STALA, ADAM PENCZEK, ANDRZEJ MONDZIK, ŁUKASZ STAWIARSKI

AGH University of Science and Technology
e-mail: stala@agh.edu.pl

Abstract: This paper presents a novel, low-complexity method of simulating PV source characteristics suitable for real-time modeling and hardware implementation. The application of the suitable model of the PV source as well as the model of all the PV system components in a real-time hardware gives a safe, fast and low cost method of testing PV systems. The paper demonstrates the concept of the PV array model and the hardware implementation in FPGAs of the system which combines two PV arrays. The obtained results confirm that the proposed model is of low complexity and can be suitable for hardware in the loop (HIL) tests of the complex PV system control, with various arrays operating under different conditions.

Key words: Photovoltaic characteristic, PV array, PV simulations, mathematical modeling, hardware in the loop (HIL)

1. Introduction

Photovoltaics (PV) is one of the most important renewable energy sources. Due to the substantial complexity of PV systems, an effective simulation tool can be advantageous for testing concepts of conversion stages, as well as control. There are many simulation methods applied for testing PV systems [1-18]. The modeling approach is also suitable for simulations of other renewable energy sources and systems [2, 5, 19-22] which can be used as components of a smart grid system [23].

PV array models generate $i(u)$, $p(u)$ according to their specific characteristics, depending on the type of array, as well as irradiance and temperature. For a system simulation, apart from PV sources, power electronic converter topologies and control are also tested in simulation applications [4, 9].

Most PV source models utilize a model of the diode [1, 3, 6-9, 11-13, 16]. Some concepts for simulating PV sources and systems are dedicated to emulate PV systems in real-time hardware (FPGA or ASIC) (Fig. 1). In PV systems, real-time simulations of PV sources make it possible to construct power supplies with PV characteristics [3, 4, 10] and to conduct laboratory tests

without using expensive solar panels. They also make it possible to set the specific operating conditions of the PV panel (e.g. in a space environment). In real-time hardware simulations (and also in PC-based simulations), a PV system is often composed of many PV arrays connected in series and parallel. Such systems become extremely complicated for real-time simulations, and a simple representation of a PV array model can become critical.

Hardware simulations can be performed for testing control on a real-time emulator of a power system implemented in an electronic chip [2-4]. Such a method is safe, fast and inexpensive, and makes it possible to carry out HIL tests. It can be more useful than PC-based simulations for verification of the operation of a targeted controller solution with a real-time object. Algorithms typical for PV systems, such as MPPT (Maximum Power Point Tracking) or anti-islanding [4] can be very effectively analyzed in an HIL system. Similarly, a problem of partial shading [2-4], of PV can be effectively tested due to the complicated control of the integrated components. The implementation of MPPT for global power peak searching under partially shaded conditions, or by individual energy conversion with MPPT and using a multi-level converter is also very important. HIL tests can be a very attractive method of testing complex, expensive systems (such as power converter systems, wind farms, driverless cars, etc.) and make it possible to reduce time and costs in comparison to field tests.

A laboratory setup for testing systems with the application of many PV arrays is very expensive, and so hardware simulation (in FPGA IC) reduces costs and makes it possible to verify conceptions for system control and topologies. In the case of a DC power supply with a PV-type output, a single PV-array characteristic is usually generated. The characteristic can be defined by a set of typical values that depends on the external conditions of PV array: U_{OC}, I_{SC}, I_{MPP}, U_{MPP}.
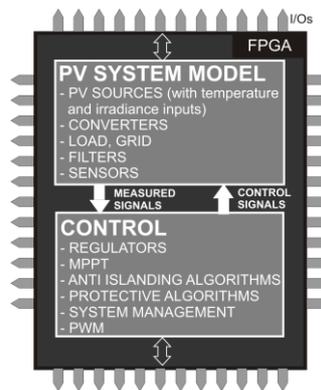

Fig. 1. An idea of FPGA-based hardware simulation
of a PV system and control verification in a real-time model

Signals generated by the model of the system implemented in the FPGA structure can be easily analyzed in the FPGA (e.g. the grid current THD or DC component). If they are used for control, the calculation procedure performed in the FPGA or DSP is verified during the simulation stage of the investigation.

This paper presents an idea for very low-complexity modeling of complex PV arrays (with many individual PV panels), published only as a patent description [17-18] so far. The concept of the model is presented analytically in Section 2. The following Section demonstrates an application of the model in FPGA-based real-time simulations.

2. FPGA-based simulation of power electronic systems

A photovoltaic system is composed of a PV source, power converters, filters and loads (as well as a control unit). Passive RLC components can create topologies that can be easily solved in real time after the discretization of any circuit equations (typical DSP algorithms should be calculated – e.g. as in [24] where an LCL AC filter was modeled). Switches (controlled and non-controlled) change the circuit topology, and their state depends on the control and the circuit conditions. The action of switches can be simulated in an FPGA as an ideal or with losses. A grid voltage waveform can be modeled with the use of algorithms of signal generation, or with the use of a table of values in a lookup table, where digital oscilloscope measurements can be used as signals in simulations.

A. Switching converters

Fig. 2 presents an idea for the construction of a PV system model.
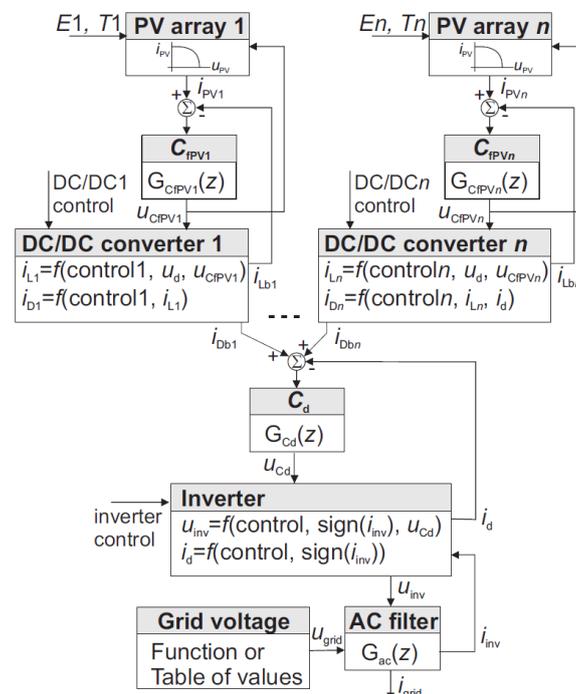

Fig. 2. Flowchart of calculation of the photovoltaic conversion system with multi DC strings and the central inverter

The system is divided into DSP blocks described by $G(z)$ transmittance and non-DSP blocks that describe the PV source, grid voltage and converters (structures with switches). The switching components can be very simply simulated as ideal switches by setting their states between zero and infinite resistance. Variations in switching states or load and sources trigger transient states in the circuit composed of passive devices. Individual L or C components can be treated as ideal or with resistances. For instance, a discrete model of a series RL circuit can be the following:

$$i(n) = i(n-1)e^{-\frac{T_p}{T}} + \frac{1}{R}u(n-1)\left(1 - e^{-\frac{T_p}{T}}\right),$$

(1)

where: $T = L/R$.

Complex circuits such as an LCL filter in a grid-connected inverter require solving a set of differential equations.

The boost converter used in the model presented is calculated in two stages, depending on the switch state (Fig. 3). These problems have been widely analyzed in the literature. As with the step-up converters various other solutions can be applied, e.g. such as the switched-capacitor boost converter presented in [25].
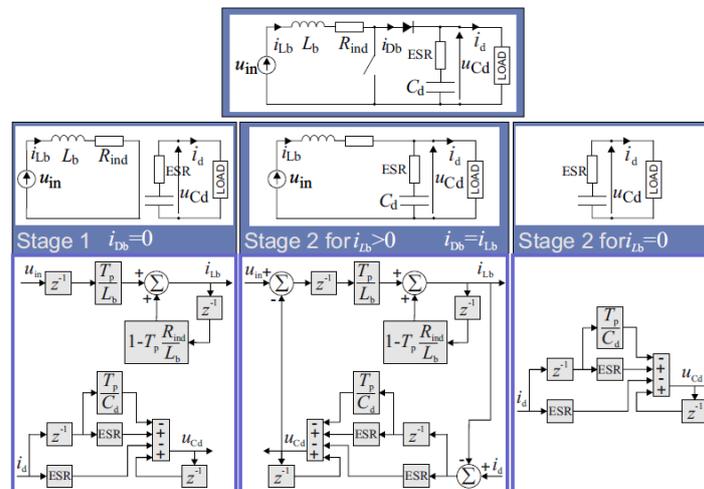

Fig. 3. The boost converter's simplified (ideal switches) discrete modeling

3. FPGA-based models of PV arrays

The most interesting component for modeling in real time is a PV array. This is a very important problem because it makes it possible to reduce the cost and time of PV system investigations and prototyping with the application of simulations. PV array models are used in

PC-based simulations, as well as in hardware simulators. The implementation of a PV array model dedicated to real time should be possible in hardware such as, for example, an FPGA. A model of a single PV array is then not supposed to use a substantial amount of resources of the FPGA, because in practical PV systems there are often many PV arrays used in various configurations.

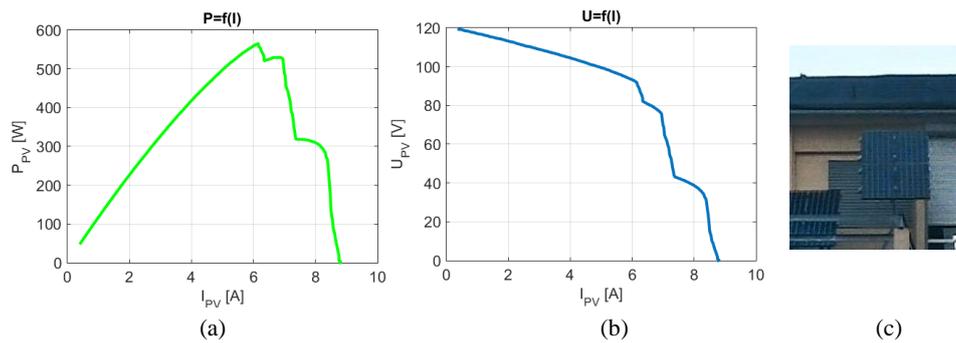(a)   (b)   (c)

Fig. 4. An example of a PV generator under the partial shaded conditions. Experimental results

The problem of modeling and control also becomes more complicated when partial shading problems occurs. The PV characteristic can have a larger number of maximum points in such case. An example of the measured characteristic of a partly shaded PV source is presented in Fig. 4. In conclusion, to achieve hardware implementation of complex PV systems for real-time emulation, a simple, effective model of a PV array is necessary.

A. A novel method of PV array modeling on the basis of a relation of two functions

A new method for real-time systems, where PV arrays characteristics are simulated, with a very simple method of approximation of $i(u)$ and $u(i)$ relations, is proposed. Fig. 5 presents a construction of a $u(i)$ characteristic as a relation between two straight lines: $(I_{SC}-i_{PV})$ and $(I_{SC}-ai_{PV})$, where $a \in R$, $a < 1$.
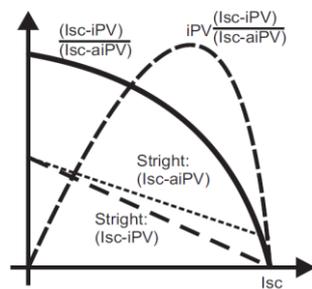

Fig. 5. A graphical representation of the construction of $u_{PV}(i_{PV})$ and $p_{PV}(i_{PV})$ [17]

The relation between the two straight lines is as follows:

$$0 \leq \frac{\left(I_{SC} - i_{PV}\right)}{\left(I_{SC} - ai_{PV}\right)} \leq 1 .$$
(2)

A basic formula for a PV array characteristic can be following:

$$u_{PV} = U_{OC} \frac{(I_{SC} - i_{PV})}{(I_{SC} - ai_{PV})}. \tag{3}$$

$$p_{PV} = u_{PV} \cdot i_{PV}. \tag{4}$$

Relation (3) complies the following conditions:

$$u_{PV} = 0 \text{ for } i_{PV} = I_{SC}, \tag{5}$$

$$u_{PV} = U_{OC} \text{ for } i_{PV} = 0. \tag{6}$$

Using more parameters in the presented construction may lead to simplification to (3):

$$u_{PV} = k U_{OC} \frac{(I_{SC} - i_{PV})}{(bI_{SC} + c - mi_{PV})}, \tag{7}$$

where: $b, c, m > 0$ and for $i_{PV} > 0$: $bI_{SC} + c - mi_{PV} > 0$.

If for $i_{PV} = 0$ the voltage u_{PV} equals U_{OC}:

$$U_{OC} = k U_{OC} \frac{(I_{SC})}{(bI_{SC} + c)} \Rightarrow (bI_{SC} + c) = kI_{SC}. \tag{8}$$

From (8) it follows that:

$$b = k, \; c = 0. \tag{9}$$

Taking (9) into consideration, (7) has the following form:

$$u_{PV} = k U_{OC} \frac{(I_{SC} - i_{PV})}{(kI_{SC} - mi_{PV})} = U_{OC} \frac{(I_{SC} - i_{PV})}{\left(I_{SC} - \frac{m}{k} i_{PV}\right)} \Rightarrow \frac{m}{k} = a. \tag{10}$$

From (10) it follows that application in (3) more parameters besides a is not necessary because it may be simplified to the basic function (3).

Equation (3) is the algebraic formula for $i(u)$ and $u(i)$ and it has two key parameters defined, I_{SC} and U_{OC}, which are related to the exposition of the PV array and temperature. The coefficient a is responsible for the shape of the $u(i)$ characteristic, which makes it possible to simulate a real PV array. Figs. 6-8 show the influence of the U_{OC}, I_{SC}, and parameters on the calculation of the u_{PV} (i_{PV}) characteristic.

There are also two important parameters set as a constraint on the PV array $u(i)$ curve simulation. These are the value of maximum power and the position of the maximum power point (MPP) on the curve. Thus, they can be set as a pair: (U_{MPP}, I_{MPP}), or (P_{MPP}, I_{MPP}), or (U_{MPP}, P_{MPP}).
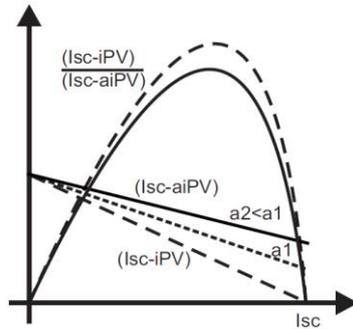
Fig. 6. An impact of the "a" coefficient
on the PV array model $p_{PV}(i_{PV})$ (3)-(4)

The parameter $a(U_{MPP})$ can be calculated as follows:

$$\frac{\mathrm{d}p_{PV}}{\mathrm{d}t} = 0 \quad \text{for} \quad I = I_{MPP},$$

(11)

$$p_{PV}(i_{PV}) = i_{PV} U_{OC} \frac{I_{SC} - i_{PV}}{I_{SC} - ai_{PV}}, \; a \in (0, 1).$$

(12)

The maximum can be found from the formula:

$$\frac{\mathrm{d}p_{PV}(i_{PV})}{\mathrm{d}i_{PV}} = U_{OC} \left[\frac{ai_{PV}^2 - 2I_{SC}i_{PV} + I_{SC}^2}{(I_{SC} - ai_{PV})^2} \right].$$

(13)

To find the maximum (the value of the current in the MPP), the zeroes of the following equation should be solved:

$$ai_{PV}^2 - 2I_{SC}i_{PV} + I_{SC}^2 = 0.$$

(14)

There are two solutions of this relation (14):

$$i_{PV1} = \frac{I_{SC}\left(1 + \sqrt{1-a}\right)}{a}, \quad a \in (0, 1)$$

(15)

for $a \in (0, 1)$ $i_{PV1} > I_{SC}$ then i_{PV1} is over the range.

$$i_{PV2} = \frac{I_{SC}\left(1 - \sqrt{1-a}\right)}{a}$$

(16)

for $a \in (0, 1)$ $i_{PV2} < I_{SC}$.

Using (16), the MPP values versus a parameter can be found:

$$i_{PVMPP} = I_{SC} \frac{1 - \sqrt{1-a}}{a},$$

(17)

$$u_{\text{PVMPP}} = U_{\text{OC}} \frac{a - (1 - \sqrt{1-a})}{a\sqrt{1-a}} .$$ (18)

From equations (17) and (18) it follows that the coefficient *a* makes it possible to fix the value of one quantity from the current, voltage or power in the MPP. The other two become a function of the parameter *a*. For example, the parameter *a* can be calculated from the desired value of the current in the maximum power point:

$$a = 2\frac{I_{\text{SC}}}{i_{\text{PVMPP}}} - \frac{I_{\text{SC}}^2}{i_{\text{PVMPP}}^2} .$$ (19)

Fig. 7 presents the variations of relative values of the current, voltage, and power of the simulated PV array as a function of the parameter *a*. Fig. 8 presents calculation results of PV array characteristic using model (3). Impact of the coefficient *a*, and U_{OC} as well as I_{SC} is also demonstrated.
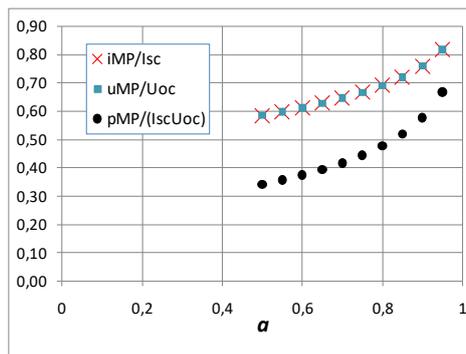

Fig. 7. The relative values of the current, voltage and power of simulated PV array
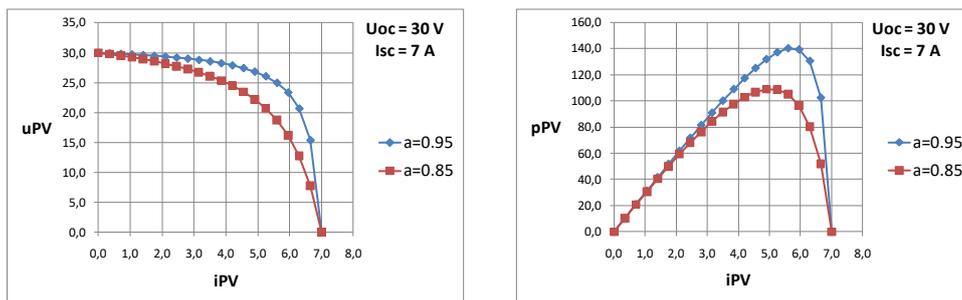as a function of the parameter *a*.

Fig. 8. An influence of *a* from (3) on calculated $u_{\text{PV}}(i_{\text{PV}})$ characteristic

The PV panel can be loaded with a device that represents a voltage source or a current source. Thus, the relations derived from (3) that describe the PV array current versus voltage are necessary. This relation can be calculated in the following way:

$$\frac{u_{\mathrm{PV}}}{U_{\mathrm{OC}}}\left(I_{\mathrm{SC}} - a \cdot i_{\mathrm{PV}}\right) = \left(I_{\mathrm{SC}} - i_{\mathrm{PV}}\right), \tag{20}$$

$$i_{\mathrm{PV}} - \frac{u_{\mathrm{PV}}}{U_{\mathrm{OC}}} \cdot a \cdot i_{\mathrm{PV}} = I_{\mathrm{SC}}\left(1 - \frac{u_{\mathrm{PV}}}{U_{\mathrm{OC}}}\right), \tag{21}$$

$$i_{\mathrm{PV}}\left(1 - \frac{u_{\mathrm{PV}}}{U_{\mathrm{OC}}} \cdot a\right) = I_{\mathrm{SC}}\left(1 - \frac{u_{\mathrm{PV}}}{U_{\mathrm{OC}}}\right), \tag{22}$$

$$i_{\mathrm{PV}} = I_{\mathrm{SC}} \cdot \frac{\left(1 - \dfrac{u_{\mathrm{PV}}}{U_{\mathrm{OC}}}\right)}{\left(1 - \dfrac{u_{\mathrm{PV}}}{U_{\mathrm{OC}}} \cdot a\right)} = I_{SC} \cdot \frac{\left(U_{\mathrm{OC}} - u_{\mathrm{PV}}\right)}{\left(U_{\mathrm{OC}} - a \cdot u_{\mathrm{PV}}\right)}. \tag{23}$$

It is remarkable that both equations (3) and (23) use the same coefficient a.

B. Additional correction of the PV curve

The parameter a makes it possible to adjust the value of the power in the MPP (P_{MPP}), but also affects I_{MPP} or U_{MPP}. In order to modify the parameters of the PV characteristic independently, additional corrections can be introduced in the basic formula. Those corrections can be achieved by a very simple modification of one or two straights used in the basic Formula (3). In the example case:

$$u_{\mathrm{PV}} = U_{\mathrm{OC}} \cdot \frac{\left(I_{\mathrm{SC}} - i_{\mathrm{PV}}\right)}{\left(I_{\mathrm{SC}} - \left(a i_{\mathrm{PV}} + CF\right)\right)}, \tag{24}$$

where: *CF* is a correcting function.

Fig. 9 and Fig. 10 present a case where a straight-type correction function (*CF*) is introduced to the PV model.
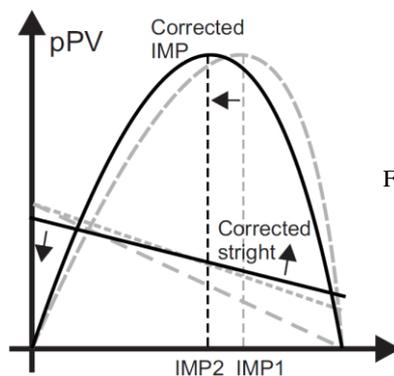

Fig. 9. Application of a straight as a correcting function (*CF*) for MPP setting

(a)

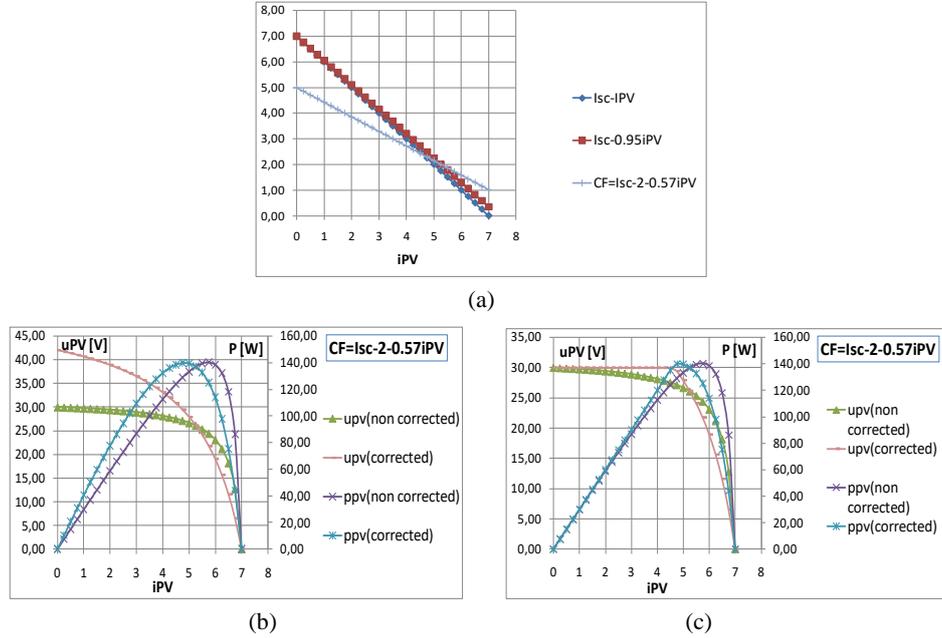
(b)   (c)

Fig. 10. Application of a correcting function $CF = I_{SC}$-2-0.57I_{PV} for MPP setting: (a) functions used in the model; (b) PV voltages and powers vs. current in the uncorrected case and the case of the use of CF function; (c) the case of correction with the PV voltage limited to U_{OC}.

C. Series and parallel connection of the PV arrays

A simulation of a series connection of PV arrays according to (3) by calculating a particular PV array voltage.

$$u_{PV} = \sum_n u_n(i_{PV}) . \tag{25}$$

Another optimized approach makes it possible to avoid *n*-times division when the total voltage is calculated. The current of the PV arrays in a series connection is the same, but the short circuit current is different in each array. Thus, the formula cannot be significantly simplified but can be converted to a solution that needs only one division, as shown in the example below:

$$u_{PV} = u_{PV1} + u_{PV2} = U_{OC1} \cdot \frac{(I_{SC1} - i_{PV})}{(I_{SC1} - a_1 i_{PV})} + U_{OC2} \cdot \frac{(I_{SC2} - i_{PV})}{(I_{SC2} - a_2 i_{PV})} , \tag{26}$$

$$u_{PV} = \frac{U_{OC1} \cdot (I_{SC1} - i_{PV}) \cdot (I_{SC2} - a_2 i_{PV}) + U_{OC2} \cdot (I_{SC2} - i_{PV}) \cdot (I_{SC1} - a_1 i_{PV})}{(I_{SC1} - a_1 i_{PV}) \cdot (I_{SC2} - a_2 i_{PV})} , \tag{27}$$

$$u_{PV} =$$
$$= \frac{U_{OC1} \cdot (I_{SC1} I_{SC2} - i_{PV}(I_{SC2} + I_{SC1} a_2) + a_2 i_{PV}^2) + U_{OC2} \cdot (I_{SC2} I_{SC1} - i_{PV}(I_{SC1} + I_{SC2} a_1) + a_2 i_{PV}^2)}{(I_{SC1} - a_1 i_{PV}) \cdot (I_{SC2} - a_2 i_{PV})} . \tag{28}$$

The relationship (28) can be calculated by using the multiplication and addition of components, and, finally a division. When one division is calculated in (28) the hardware (e.g. FPGA) resources can be saved using (28) instead of (26). This leads to the conclusion that the proper preparation of a calculation performed in real time (at the model creation stage) can make substantial savings on hardware resources possible. The calculation of parallel systems can be analyzed in the same way. The difference is that the parallel branches have the same voltage at terminals.

4. Real time hardware implementation of the PV array model

The proposed model represents an algebraic function between u_{PV} and i_{PV}. Thus, a recurrence calculation or lookup table searching is not needed, and so the method is very fast, and resource efficient. In this way, simulating a single PV source, even in a real-time emulator, is very simple and efficient. However, most PV systems utilize strings of PV arrays in series or parallel configuration.

In real time systems, the speed of calculating the *U/I* characteristic can be critical for the emulator. Where necessary, the PV array parameters can be calculated using an independent, digital part of the resources for each PV source. The first table and Fig. 11 present an example of the implementation of a single $u_{PV}(i_{PV})$ characteristic according to (3). The system is modeled with the use of fixed-point arithmetic with 10-bit precision (Fig. 12).

In order to save resources, the most resource-demanding part of the model, namely the divider, can be shared for various instances. A sample concept of such a solution is presented in Fig. 12, where two models of a PV *U/I* characteristic are calculated with the use of a single divider. In general, when the time of calculating a PV *U/I* characteristic is achieved shorter than demand, the method which utilizes the available resources, may be used to provide many different calculations. In such a case, the PV array algorithm can be used many times in the overall calculation cycle, using different parameters to calculate the characteristics of many PV arrays. This solution can provide a very efficient utilization of resources and can be used for PV plant simulations. The simulation model was also verified in the debugging tool. Fig. 13 presents waveforms of a system composed of two PV arrays connected in series.
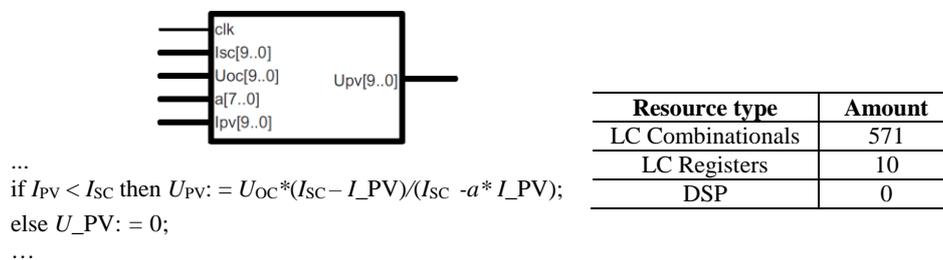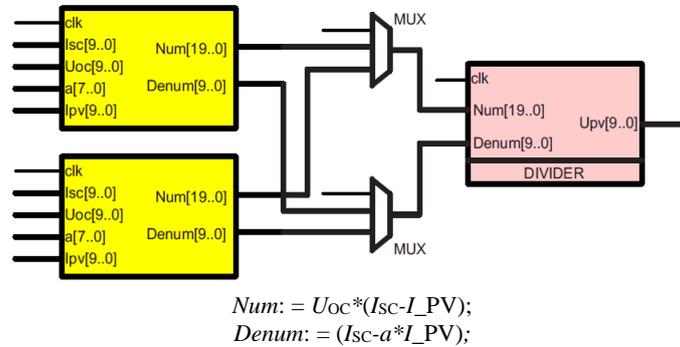

...
if $I_{PV} < I_{SC}$ then U_{PV}: = $U_{OC}*(I_{SC} - I\_PV)/(I_{SC} -a* I\_PV)$;
else U_PV: = 0;
…

Resource type	Amount
LC Combinationals	571
LC Registers	10
DSP	0

Fig. 11. Resources usage in the simplest approach for VHDL calculation of a single PV *U/I* characteristic. FPGA Cyclone III resources for 10 b resolution, commutated with 50 ns VHDL-based process

$$Num: = U_{OC} * (I_{SC} - I\_PV);$$
$$Denum: = (I_{SC} - a * I\_PV);$$

	Resource type	Amount
Numerator/ Denumerator	LC Combinational LC Registers	11 30
Mux	LC Combinational LC Registers	10 10
Divider	LC Combinational LC Registers	334 30

Fig. 12. Resources usage in the simplest approach for VHDL calculation of a single PV *U/I* characteristic. FPGA Cyclone III resources for 10 b resolution for input and output signals with internal 20 b numerators. 50 ns clock period
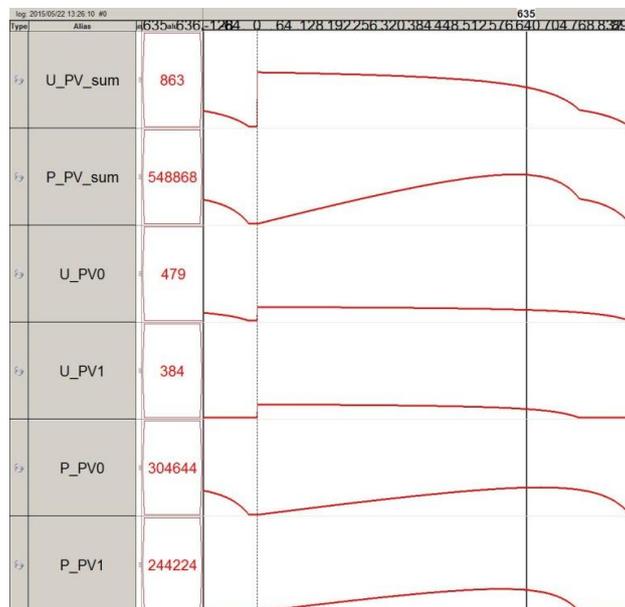

Fig. 13. FPGA-based real-time simulation results of the system composed from two series connected PV arrays. Results plotted in Signal Tap Logic Analyzer in Quartus software

It is evident that complex characteristics with local maxima can be adequately simulated, which can be suitable for tests of control algorithms such as MPPT.

Conclusion

In this paper, a concept of a very low-complexity mathematical model of PV source characteristics was presented. In the model, the basic parameters of the PV characteristics (such as open circuit voltage, short-circuit current, and MPP power) are defined. The model is suitable for real-time hardware simulation, as confirmed using an FPGA-based implementation of the model. In complex PV array systems, the proposed model can be simplified to achieve a reduction in the hardware resources required. A further modification of the basic formula makes it possible to program parameters in the maximum power point. On the basis of tests of the implementation of the proposed model in the FPGA hardware, the following conclusions can be also confirmed:

– it is possible to verify the control of complex systems without the application of power components (PV source, converters, filters, grid),
– control algorithms can be tested in a dedicated device (e.g. FPGA, DSP, analog),
– failure states and protective algorithms can be tested safely,
– the effects of environmental conditions (e.g. irradiation, temperature) on the analyzed system can be tested easily,
– the method can be applied in systems with other renewable energy sources,
– the PV array characteristics generated can be refreshed with megahertz frequency (a single PV model can be used by many converters having different parameters),
– signals from the model (e.g. grid current) can be analyzed in real time in the same FPGA,
– debugging tools make it possible to observe many signals simultaneously (more so than with the use of scope measurements).

For further improvements and utilization of resources, a more effective division should be implemented.

References

[1] Villalva M.G., Gazoli J.R., Filho E.R., *Comprehensive Approach to Modeling and Simulation of Photovoltaic Arrays*, IEEE Trans. on Power. Electron., vol. 24, pp. 1198-1208 (2009).
[2] Parera Ruiz A., Cirstea M., Koczara W., Teodorescu R., *A novel integrated renewable energy system modelling approach, allowing fast FPGA controller prototyping*, 2008 11th International Conference on Optimization of Electrical and Electronic Equipment, Brasov, pp. 395-400 (2008).
[3] Koutroulis E., Kalaitzakis K., Tzitzilonis V., *Development of an FPGA-based System for Real-Time Simulation of Photovoltaic Modules*, Seventeenth IEEE International Workshop on Rapid System Prototyping (RSP'06), Chania, Crete, pp. 200-208 (2006).
[4] Stala R., *Testing of the grid-connected photovoltaic systems using FPGA-based real-time model*, 13th Int. Power Electronics and Motion Control Conference, Poznan, Poland (2008).
[5] Stala R., Stawiarski L., *Real-time models of PV arrays implemented in FPGAs*, Przeglad Elektrotechniczny (in Polish), vol. 86, no. 2, pp. 358-363 (2010).
[6] Maffezzoni P., Codecasa L., D'Amore D., *Modeling and Simulation of a Hybrid Photovoltaic Module Equipped With a Heat-Recovery System*, IEEE Trans. on Ind. Elec., vol. 56, pp. 4311-4318 (2009).

 [7] Vitorino M.A., Hartmann L.V., Lima A.M.N., Corrêa M.B.R., *Using the model of the solar cell for determining the maximum power point of photovoltaic systems*, 12th European Conference on Power Electronics and Applications EPE'07, CD Proceedings (2007).

 [8] Böke U., *A simple model of photovoltaic module electric characteristics*, 12th European Conference on Power Electronics and Applications EPE'07, CD Proceedings (2007).

 [9] Midtgard O.M., *A simple photovoltaic simulator for testing of power electronics*, 12th European Conference on Power Electronics and Applications EPE'07, CD Proceedings (2007).

[10] Raposa G., *Testing Terrestrial Solar-powered Inverters Using Solar Array Simulation Techniques*, Agilent Technologies, Inc. (2009).

[11] Ma J., Bi Z., Ting T.O., Hao S., Hao W., *Comparative performance on photovoltaic model parameter identification via bio-inspired algorithms*, Solar Energy, vol. 132, pp. 606-616 (2016).

[12] Lun S-x., Wang S., Yang G-h., Guo T-t., *A new explicit double-diode modeling method based on Lambert W-function for photovoltaic arrays*, Solar Energy, vol. 116, pp. 69-82 (2015).

[13] Park J-Y., Choi S-J., *A novel datasheet-based parameter extraction method for a single-diode photovoltaic array model*, Solar Energy, ISSN 0038092X, vol. 122, p. 1235 (2015).

[14] Mahmoud Y., El-saadany E., *Accuracy comparison between Gompertz and polynomial based PV models*, Smart Energy Grid Engineering (SEGE), 2015 IEEE International Conference on, Oshawa, Canada, pp. 1-4. (2015), DOI: 10.1109/SEGE.2015.7324616.

[15] Dash S.K., Raj R.A., Nema S., Nema R.K., *A quantitative and comparative performance evaluation of PV models on PSPICE platform*, Circuit, Power and Computing Technologies (ICCPCT), 2015 International Conference on, Nagercoil, pp. 1-8 (2015), DOI: 10.1109/ICCPCT.2015.7159479.

[16] Shongwe S., Hanif M., *Comparative Analysis of Different Single-Diode PV Modeling Methods*, IEEE Journal of Photovoltaics, vol. 5, no. 3, pp. 938-946, (2015), DOI: 10.1109/JPHOTOV. 2015.2395137.

[17] Stala R., *Simulation method and system for simulation the current-voltage characteristics of the photovoltaic cell*, Patent PL 222545 B1 (2016).

[18] Stala R., *Simulation method and system for simulation the voltage-current characteristics of the photovoltaic cell*, Patent PL 222546 B1 (2016).

[19] Szkolny S., Małyszko O., *Hardware-in-the-loop simulator for testing wind turbine generators*, Zeszyty Problemowe – Maszyny Elektryczne, vol. 3, no. 103, pp. 269-274 (2014).

[20] Szkolny S., Małyszko O., *Hardware-in-the-loop simulator for testing wind turbine generators*, Czasopismo Techniczne. Elektrotechnika – Technical Transactions. Electrical Engineering R. 112, vol. 1-E, no. 8, pp. 229-239 (2015).

[21] Baszyński M., *Low cost, high accuracy real-time simulation used for rapid prototyping and testing control algorithms on example of BLDC motor*, Archives of Electrical Engineering, ISSN (Online) 2300-2506, vol. 65, no. 3, pp. 463-479 (2016), DOI: 10.1515/aee-2016-0034.

[22] Baszyński M., *A model of the single-phase multicell rectifier with sinusoidal source current using FPGA implementation*, Przegląd Elektrotechniczny, vol. 85 no 10, pp. 76-82 (2009).

[23] Khalil S.S., Abu-Rub H., *Smart Grid Condition Assessment: Concepts, Benefits, and Developments*, Power Electronics and Drives 1, vol. 36, no. 2 (2016).

[24] Mariéthoz S., Morari M., *Explicit Model-Predictive Control of a PWM Inverter with an LCL Filter*, IEEE Trans. on Ind. Electron., vol. 56, no. 2, pp. 389-399 (2009).

[25] Mondzik A., Waradzyn Z., Stala R., Penczek A., *High efficiency switched capacitor voltage doubler with planar core-based resonant choke*, 2016 10th International Conference on Compatibility, Power Electronics and Power Engineering (CPE-POWERENG), Bydgoszcz, pp. 402-409 (2016).

[26] Waradzyn Z., Stala R., Mondzik A., Pirog S., *Switched Capacitor-Based Power Electronic Converter-Optimization of High Frequency Resonant Circuit Components*, in Advanced Control of Electrical Drives and Power Electronic Converters, ser. Studies in Systems, Decision and Control, Springer International Publishing AG, pp. 361-378 (2017).